Geophysical Research Letters

RESEARCH LETTER
10.1029/2020GL087585

Internal Variability Dominates Over Externally Forced Ocean Circulation Changes Seen Through CFCs

J. G. Lester[1], N. S. Lovenduski[2], H. D. Graven[1], M. C. Long[3], and K. Lindsay[3]

[1]Department of Physics and Grantham Institute, Imperial College London, London, UK, [2]Department of Atmospheric and Oceanic Sciences and Institute of Arctic and Alpine Research, University of Colorado Boulder, Boulder, CO, USA, [3]Climate and Global Dynamics Laboratory, National Center for Atmospheric Research, Boulder, CO, USA

Key Points:
- A model ensemble analysis indicates that externally forced ocean circulation changes from 1991 to 2005 are smaller than internal variability
- The changes in modeled CFC12 between 1991 and 2005 are subject to large internal variability
- Large internal variability in oceanic tracer changes challenges our ability to detect forced changes in circulation from these tracers

Supporting Information:
- Supporting Information S1

Correspondence to:
J. G. Lester,
j.lester16@imperial.ac.uk

Citation:
Lester, J. G., Lovenduski, N. S., Graven, H. D., Long, M. C., & Lindsay, K. (2020). Internal variability dominates over externally forced ocean circulation changes seen through CFCs. *Geophysical Research Letters*, *47*. https://doi.org/10.1029/2020GL087585

Received 18 FEB 2020
Accepted 11 APR 2020
Accepted article online 23 APR 2020

Abstract Observations of oceanic transient tracers have indicated that the circulation in the Southern Ocean has changed in recent decades, potentially driven by changes in external climate forcing. Here, we use the CESM Large Ensemble to analyze changes in two oceanic tracers that are affected by ocean circulation: the partial pressure of chlorofluorocarbon-12 (pCFC12) and the idealized model tracer Ideal Age (IAGE) over the 1991 to 2005 period. The small ensemble mean change in IAGE suggests that there has been very little externally forced change in Southern Ocean circulation over this period, in contrast to strong internal variability. Further, our analysis implies that real-world observations of changes in pCFC12 may not be a robust way to characterize externally driven changes in Southern Ocean circulation because of the large internal variability in pCFC12 changes exhibited by the individual ensemble members.

Plain Language Summary It is important to understand how the circulation of the Southern Ocean responds to external factors, such as changing surface winds. Circulation changes are difficult to measure over such a large scale, but we can infer changes by looking at the spreading and mixing of tracers in the ocean. Recent studies using the tracer chlorofluorocarbon-12 (CFC12) have found evidence that the Southern Ocean circulation changed from the 1990s to the 2000s. Our study uses a computer model which simulated the twentieth century oceanic uptake of CFC12, many times over, providing a statistical spread of the internal variability of the ocean. We compared the modeled CFC12 evolution to real-world observations, along with a second model tracer called Ideal Age which we use to detect circulation changes. The model results suggest that the changes we observe in CFC12 from 1991 to 2005 are dominated by internal variability, or noise, rather than coherent circulation change, as measured by Ideal Age. The results indicate that human-induced trends in ocean circulation in some regions will only be detectable over periods longer than one or two decades.

1. Introduction

The circulation of the Southern Ocean sets the state for its important role in the climate system. Persistent westerly winds transport old circumpolar deep water (CDW) to the surface at the high latitudes and subduct Subantarctic Mode Water (SAMW) and intermediate water masses to the ocean interior at lower latitudes (Rintoul & Naveira Garabato, 2013). This meridional overturning circulation is tightly coupled to the fluxes of carbon and heat at the air-sea interface (Lovenduski et al., 2007; Russell et al., 2006) and affected by the strength of the westerly winds (Hall & Visbeck, 2002; Lovenduski & Gruber, 2005).

Several studies based on transient oceanic tracers have suggested that the circulation of the Southern Ocean has changed with time. Waugh et al. (2013) used repeat CFC12 hydrographic transects in the Southern Ocean to infer that upwelling of CDW and subduction of SAMW had increased from the 1990s to the 2000s. Tanhua et al. (2013) exploited the 14 year time lag in atmospheric increase rates of CFC12 and sulfur hexafluoride (SF6) and found similar changes in ventilation in the South Pacific Ocean as Waugh et al. (2013), but conversely no evidence of change in the South Indian Ocean. More recently, Ting and Holzer (2017) found coherent decadal changes in Southern Ocean ventilation, broadly consistent with those identified by Waugh et al. (2013). In summary, these transient tracer studies indicate an acceleration in Southern Ocean meridional overturning from the 1990s to the 2000s.

Studies intimate that this acceleration in meridional overturning is driven by an externally forced change in the climate system, namely, the strengthening westerly winds over the Southern Ocean in association with

stratospheric ozone depletion (Gillett & Thompson, 2003; McLandress et al., 2011; Polvani et al., 2011; Thompson et al., 2011). These studies suggest only a small role for internal variability (the unforced intrinsic variability in the climate system) in the circulation changes. Attribution of change will help us understand the system, which might ultimately feedback to our ability to predict the future evolution of Southern Ocean heat and carbon absorption (e.g., DeVries et al., 2017; Le Quéré et al., 2007; Lovenduski et al., 2008). Shao et al. (2016) highlight the limitations for using CFC12 in 1-D models to identify trends in ventilation, outside of the subtropical thermocline. A further complication in transient tracer studies is that the observations are typically only collected every 10 years or so (Talley et al., 2016), limiting our ability to use these tracers to fully characterize the variable ocean circulation on shorter timescales and to attribute these changes to external forcing or internal variability.

Here, we use a novel large ensemble modeling approach to gain insight on recent variability and changes in CFC12 concentrations in the Southern Ocean between 1991 and 2005. The large ensemble provides an assessment of the model's response to historical forcings and an evaluation of internal (unforced) variability. We find that the forced changes in CFC-derived estimates of Southern Ocean circulation are small relative to the spread across the ensemble, suggesting that internal variability plays a large role in observed changes.

2. Methods

2.1. Ocean Observations

We compare pCFC12 from ship-based observations in the 1990s and 2000s from the repeat hydrography section at P16S (150°W), taken from the GLODAPv2 database (Key et al., 2015; Olsen et al., 2016). Two other sections (A16 and I08S/I09N) are presented in the supporting information, along with the full meridional extent of P16, and a summary of the observations is given in Table S1.

To compare observations made in the 1990s and 2000s at slightly different locations in latitude and depth, and to account for vertical heave in isopycnals, we bin the observations by potential density (σ_θ) and latitude. The bin widths are approximately 2° in latitude and between 0.2 and 1 potential density units, which approximately matches the vertical resolution of the samples. Then we average the values in each bin, an approach used in other ocean tracer studies (Fine et al., 2017; Graven et al., 2012). Concentrations lower than 2 ppt were excluded to remove noise at the transition from low to zero concentration. The observed pCFC12 section along P16S in 1991 is shown in Figure 1a, and the change in pCFC12 from 1991 to 2005 (ΔpCFC12) is shown in Figure 1c. Concentration sections are plotted against potential density in Figure 1 and against depth in Figure S1.

2.2. Ocean Model Simulations

We use output from the historical period (1920 to 2005) of the Community Earth System Model Large Ensemble (CESM-LE; Kay et al., 2015; see also Deser et al., 2016). The ensemble comprises 34 members, each an individual simulation of the CESM version 1 (CESM) coupled atmosphere-ocean-land-ice model. The ensemble members are commonly forced with identical radiative and atmospheric histories (including the observed evolution of CFC12) but differ by a tiny perturbation to the initial air temperature in 1920 (Kay et al., 2015). A single control run was forced with preindustrial (1850) conditions for 1,800 years. The first ensemble member starts from a randomly selected year of the control run, year 402, which is assigned the year 1850 and integrated forward using historical forcing to the year 2005. The remaining 33 members were started from year 1920 of ensemble member 1, perturbed by slightly different initial conditions. The ocean component of CESM was integrated at approximately 1° horizontal resolution with 60 vertical layers (Smith et al., 2010). The mean across the 34-member ensemble provides a robust estimate of both the forced signal, that is, the change shared by all members, and the internal (unforced) variability, that is, the spread across the ensemble members.

Modeled monthly CFC12 concentrations were converted to pCFC12 using the standard solubility formulation (Warner & Weiss, 1985), and annual means were calculated for 1991 and 2005. Modeled CFC12 values were remapped from their original depth vertical coordinate to potential density.

A typical approach to separating the effects of atmospheric history and the effects of changing circulation on ΔpCFC12 uses model simulations with fixed circulation (e.g., Waugh et al., 2013). A fixed circulation simulation is not available for CESM, so we investigate changes to ocean circulation using Ideal Age (IAGE).

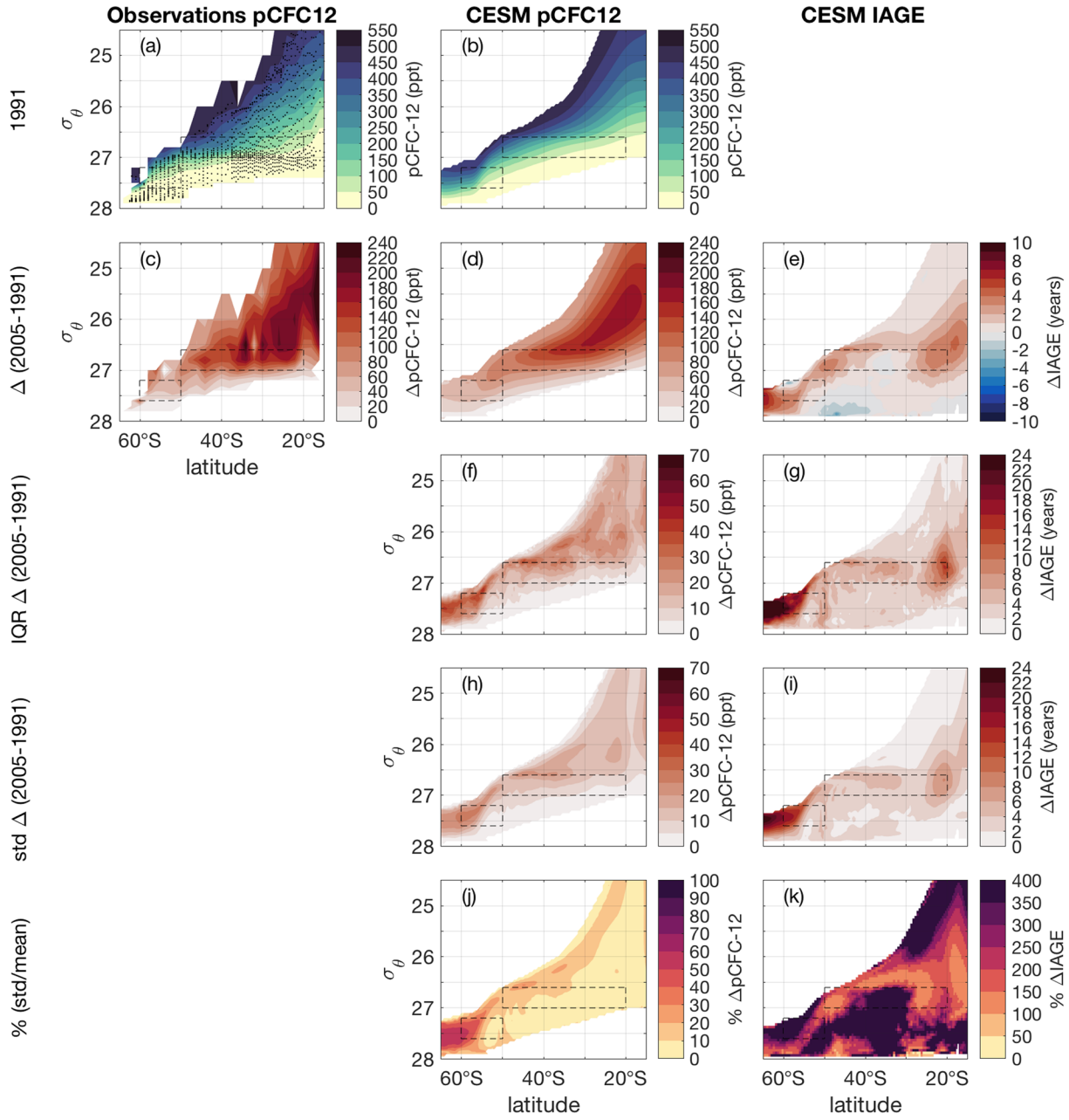

Figure 1. Potential density sections along P16S in observations and model ensemble. (a) Observed pCFC12 in 1991 where black dots show sample locations, (b) CESM-LE annual average $pCFC12_{LEav}$, (c) observed ΔpCFC12 from 1991 to 2005, (d) CESM-LE average $\Delta pCFC12_{LEav}$ from 1991 to 2005, (e) CESM-LE average $\Delta IAGE_{LEav}$ from 1991 to 2005, (f) CESM-LE interquartile range $\Delta pCFC12_{LEiqr}$, (g) CESM-LE interquartile range $\Delta IAGE_{LEiqr}$, (h) CESM-LE standard deviation $\Delta pCFC12_{LEstd}$, (i) CESM-LE standard deviation $\Delta IAGE_{LEstd}$, (j and k) the standard deviation divided by the average, $\Delta pCFC12_{LE\%}$ and $\Delta IAGE_{LE\%}$, respectively. Dashed boxes define regions used for water mass calculations, where lower left box is CDW and upper right box is SAMW.

IAGE is an idealized passive ocean tracer that records the length of time since a parcel of water was last in contact with the atmosphere at the ocean surface; thus, deeper water is typically "old," and recently ventilated waters are "young." IAGE is initialized as zero everywhere at the start of the control run and then increases by 1 year each year. It is reset to zero in surface grid boxes every year (Smith et al., 2010). The IAGE results presented here have been corrected for model drift, see supporting information. IAGE annual averages were calculated from modeled monthly outputs in the same way as pCFC12 and remapped from their original depth vertical coordinate to potential density.

As IAGE does not have a time-varying atmospheric history (unlike CFCs), it can be used to investigate temporal changes in modeled ocean circulation. We present this relationship formally in the following equations using C as a placeholder for a generic tracer concentration (either IAGE or pCFC12). For each *n* member, the total change in distribution of C from 1991 to 2005 (ΔC_{nTOT}) is a combination of ocean circulation in response to external forcing (ΔC_{nEF}), circulation changes driven by internal variability (ΔC_{nIV}), and the changing atmospheric boundary (ΔC_{nAB}), where $\Delta C_{nAB} = 0$ for IAGE:

$$\Delta C_{nTOT} = \Delta C_{nEF} + \Delta C_{nIV} + \Delta C_{nAB}. \quad (1)$$

The ensemble average of ΔC_{nTOT} across all 34 members, ΔC_{LEav}, is therefore equal to the externally forced change between 1991 and 2005 for IAGE (Figure 1e) and the combination of externally forced change and changing atmospheric boundary for pCFC12 (Figure 1d). We similarly calculate the ensemble interquartile range ΔC_{LEiqr} (Figures 1f and 1g) and the ensemble standard deviation across all 34 members, ΔC_{LEstd} (Figures 1h and 1i). We define the internal variability anomaly for each member as the difference from the ensemble average, following

$$\Delta C_{nIV} = \Delta C_{nTOT} - \Delta C_{LEav}. \quad (2)$$

We then examine the magnitude of the tracer standard deviations as a percentage of the ensemble average (Figures 1j and 1k), also known as the coefficient of variation (e.g., Fyke et al., 2017):

$$\Delta C_{LE\%} = \Delta C_{LEstd} / |\Delta C_{LEav}| \times 100\%. \quad (3)$$

To explore changes in pCFC12 outside the Southern Ocean we present the depth and value of maximum $\Delta pCFC12_{LEav}$ at each modeled latitude and longitude across the global ocean. At the depth of maximum $\Delta pCFC12_{LEav}$, we assess internal variability in ΔpCFC12 by calculating the standard deviation across the ensemble and its magnitude as a percentage of the ensemble average, as described in equation (3).

We use pCFC12 and IAGE as independent tracers, as they are each sensitive to different parts of the age distribution of a water mass. We use the ensemble mean change in ideal age to track forced changes in circulation, not forced changes in ΔpCFC12. We track forced changes in pCFC12 from the large ensemble mean. We note that ΔIAGE and ΔpCFC12 are highly correlated (Figure S4) and that previous studies have found agreement between them (Fine et al., 2017; Waugh et al., 2013, 2019). In downwelling SAMW, a negative ΔIAGE implies an increase in downwelling, as young recently ventilated water is transported to depth more quickly or in greater volume. A positive ΔIAGE in downwelling SAMW implies a decrease in downwelling. In upwelling CDW, a positive ΔIAGE implies an increase in upwelling, and a negative ΔIAGE implies a decrease. Positive and negative ΔpCFC12s have the opposite meaning to those described for ΔIAGE.

We define internal variability as the chaotic variability each ensemble member experiences as a result of its initial condition perturbation, characteristic of a random stochastic process (Deser et al., 2012). This is different from natural variability, which includes these random stochastic processes but also all natural external forcings such as volcanic eruptions. We define external forcing to include both anthropogenic forcing and natural external forcings like volcanoes.

3. Results

Observations of pCFC12 in 1991 on P16S (Figure 1a) show maximum concentrations of 550 ppt at the surface, with concentrations decreasing with depth and potential density. The ΔpCFC12 from 1991 to 2005 (Figure 1c) shows an increase in pCFC12 across the entire section, as previously shown in Fine (2011), Waugh et al. (2013), and Ting and Holzer (2017). The strongest increases are seen in the lighter more northerly waters, but we observe average increases in SAMW of 140 ppt, and 50 ppt in CDW.

The modeled $\Delta pCFC12_{LEav}$ (Figure 1d) broadly agrees with the observations (Figure 1c). The modeled $pCFC12_{LEav}$ and $\Delta pCFC12_{LEav}$ magnitudes are lower than observed, consistent with studies showing that the uptake of ocean tracers in CESM is sluggish (Long et al., 2013). CESM-LE predicts a smaller

ΔpCFC12 in the SAMW region than the observations (an average of 40 ppt lower), while the modeled ΔpCFC12 in the CDW region generally agrees well with the observations (within ±6 ppt on average).

We quantify the role of internal variability in changing pCFC12 over 1991–2005 by plotting the interquartile range and the standard deviation in this difference across the 34 members ($\Delta pCFC12_{LEiqr}$ and $\Delta pCFC12_{LEstd}$; see section 2). Both measures of variability are spatially correlated, implying the ensemble has not generated significant outliers. Across much of the section, the internal variability represents less than 10% of the ensemble mean (Figure 1j), but we note three regions along P16S which exhibit particularly high internal variability. First in southern CDW, $\Delta pCFC12_{LEstd}$ approaches a maximum of 26 ppt compared to an average $\Delta pCFC12_{LEstd}$ of 55 ppt, meaning the maximum internal variability is over 50% of the ensemble mean change (Figure 1j). This region of higher variability is likely a response to the differing upwelling rates of CDW across the ensemble, as evidenced by the high $\Delta IAGE_{LEstd}$ at the same location (Figure 1k). The same pattern is seen when binning with depth rather than potential density (Figures S1h and S1i). High internal variability is also observed in the SAMW region between 50°S and 20°S centered around the 26.6 σ_θ surface. $\Delta pCFC12_{LEstd}$ here is up to 25 ppt, but this is also the region of highest $\Delta pCFC12_{LEav}$, so that $\Delta pCFC12_{LEstd}$ represents up to a maximum of 30% of $\Delta pCFC12_{LEav}$ (similar results are seen against depth, Figure S1j). Finally, in the lighter waters (25.0 kg/m^3 < σ_θ < 26.5 kg/m^3) either side of 20°S we see the edge of another elevated region of variability, corresponding to the Pacific South Equatorial Current. In summary, we find that internal variability influences pCFC12 changes along P16S, in particular in the CDW upwelling and SAMW subduction regions.

Significant increases or decreases in IAGE can imply changes in modeled ocean circulation. The ensemble mean change in IAGE from 1991 to 2005 ($\Delta IAGE_{LEav}$, Figure 1e), which represents the forced change due to external factors, generally shows water is increasing in age across the section. IAGE increases in both SAMW and CDW by an average of +2 years (see supporting information for details on water mass calculations). However, in these same water masses, the average $\Delta IAGE_{LEstd}$ is on average 4.5 years, indicating that internal variability is larger than the forced trend. The average internal variability of ΔIAGE as a percentage of the ensemble average, $\Delta IAGE_{LE\%}$, is larger than 750% in CDW and SAMW, and more than 50% across the whole section (Figures 1k and S1k). This suggests a large role for internal variability in the observed Southern Ocean circulation changes over 1991 to 2005.

The majority of high values of $\Delta IAGE_{LE\%}$ are where changes in $\Delta IAGE_{LEav}$ are close to zero (Figures 1e and 1k). However, the high values in $\Delta IAGE_{LE\%}$ around the isopycnal outcropping region of CDW are due to elevated $\Delta IAGE_{LEstd}$, which reflects the sensitivity of ΔIAGE to changes in ventilation and upwelling (Figures 1g, 1i, 2b, and 2d).

We illustrate the linkages between changes in pCFC12 and IAGE by comparing $\Delta pCFC12_{nIV}$ and $\Delta IAGE_{nIV}$ in two ensemble members (Figures 2 and S3). There was an anomalous increase in CDW ΔpCFC12 (up to +60 ppt) in member 1 (Figure 2a) and an anomalous decrease (up to −65 ppt) in member 27 (Figure 2c). There was an anomalous increase in SAMW ΔpCFC12 (up to +40 ppt) in member 1 and an anomalous decrease (up to −25 ppt) in member 27. A strong negative correlation between ΔpCFC12 and ΔIAGE is apparent in these selected members, as well as in correlations calculated across all ensemble members (Figure S4), indicating that circulation changes in CDW and SAMW explain the anomalies in ΔpCFC12. Although SAMW and CDW ideal age changes in the ensemble members selected for Figure 2 happen to covary with the same sign, that is not the case across the ensemble, where ideal age changes increase and decrease in all combinations per water mass (Figure S5).

We can use the anomalous changes in IAGE to explain the different circulation behavior and ΔpCFC12 in the two ensemble members. In the ensemble mean, CDW IAGE increased slightly, implying increased upwelling of deep, old waters (Figure 1e). The change in CDW IAGE in member 1 is negative (up to 30 years lower than the ensemble mean; Figure 2b), implying upwelling has decreased over the observation period. The opposite occurs in member 27 (Figure 2d) where the change in CDW IAGE is anomalously positive (by up to 40 years), indicating upwelling has increased more strongly in this member. Enhanced upwelling in CDW corresponds to more entrainment of deep, low-CFC water and thus weaker increases in pCFC12 (Waugh et al., 2013), as shown in Figure 2c, whereas reduced upwelling in CDW corresponds to stronger increases in pCFC12 (Figure 2a). In SAMW, the ensemble mean $\Delta IAGE_{LEav}$ is slightly positive

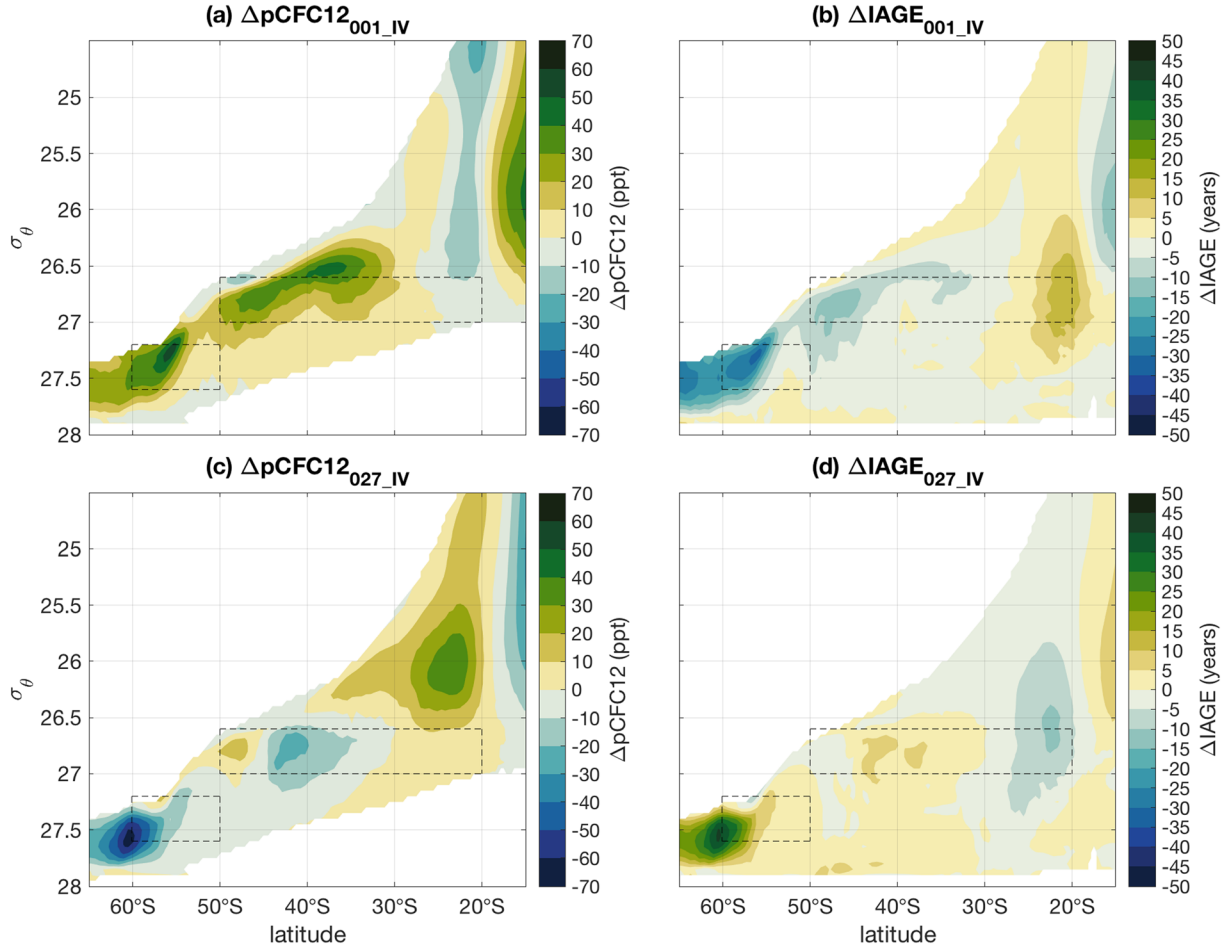

Figure 2. Potential density sections along P16S for (a) $\Delta pCFC12_{nIV}$ for ensemble member 1 and (c) member 27, (b) $\Delta IAGE_{nIV}$ for ensemble member 1 and (d) member 027. Dashed boxes define regions used for water mass calculations, where lower left box is CDW and upper right box is SAMW.

(Figure 1e), indicating a reduction in downwelling. IAGE decreases in member 1, corresponding to an increase in downwelling and a greater increase in pCFC12 as more high-CFC surface water is downwelled (Waugh et al., 2013). Weaker downwelling in member 27 (Figure 2d) corresponds to weaker increases in pCFC12 (Figure 2c). This demonstrates the internal variability in the ensemble results in vastly different circulation changes with time. Extending this analysis to additional meridional sections demonstrates that strong internal variability relative to forced circulation change is not unique to the Southern Ocean (Figures S6, S7, and S8). There is little evidence of circulation change in $\Delta IAGE_{LEav}$ (Figures S6e, S7e, and S8e), but we see high variability in ΔpCFC12 and ΔIAGE focused in the Southern Ocean, the North Pacific, and around the equator (Figures S6h and S6i).

Finally, we look more broadly at the global ocean (Figure 3). The depth of the maximum ΔpCFC12 varies from 300–600 m in the south Pacific, Atlantic, and Indian oceans to between 2,000 and 4,500 m in the North Atlantic (Figure 3a). The depth of maximum ΔpCFC12 in the equatorial region is much closer to the surface, at depths of 200 m or shallower (Figure 3a). The depth of maximum $\Delta pCFC12_{LEav}$ was found to be very similar to the depth of maximum $\Delta pCFC12_{LEstd}$. The highest values of $\Delta pCFC12_{LEav}$ are seen in the deep North Atlantic, and at a depth of around 500 m in the eastern South Pacific and the western Indian Ocean, where maximum modeled values reach around 215 ppt (Figures 1e and 3b). Compared to P16S, the internal variability as a proportion of the ensemble mean is much higher in the equatorial region, in the North Pacific Subpolar Gyre, and along the southern edge of the Antarctic Circumpolar Current. In these regions $\Delta pCFC12_{LEav}$ is smaller and much closer to the surface, and high variability is likely caused by variations in wind-driven mixing (Figure 3d).

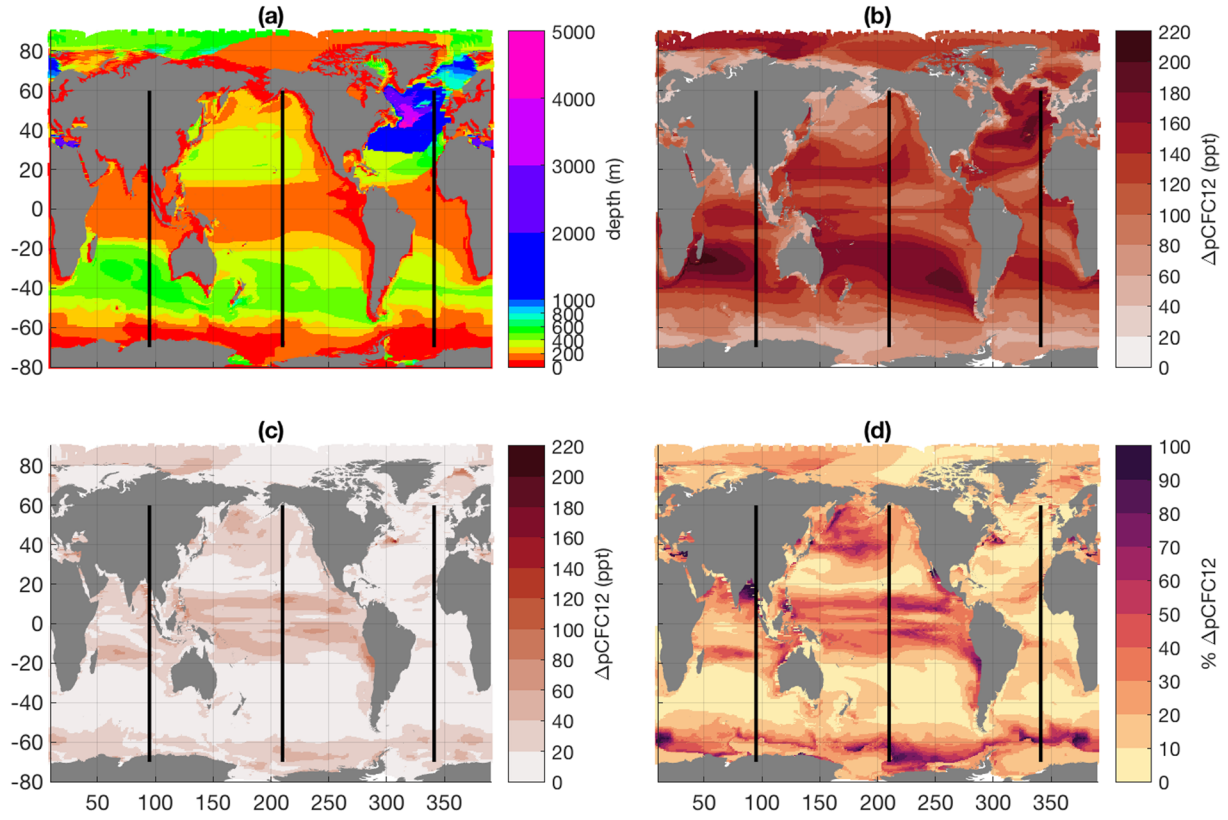

Figure 3. Global maps showing (a) depth of maximum $\Delta pCFC12_{LEav}$, (b) the value of the maximum $\Delta pCFC12_{LEmax}$, (c) the standard deviation of the maximum ΔpCFC12 across 34 members at the depth in (a), and (d) the percentage of the maximum $\Delta pCFC12_{LEstd}$ divided by the average $\Delta pCFC12_{LEmax}$ at the same depth as (a). Lines show the approximate location of hydrographic sections plotted in Figures 1 and S6–S8.

4. Discussion

The CESM Large Ensemble simulations show that the effect of internal variability in ocean circulation on ΔpCFC12 and ΔIAGE is larger than the effect of forced changes in circulation. These findings are relevant to studies which determine circulation change based on decadal hydrographic transects (DeVries et al., 2017; Ting & Holzer, 2017; Waugh et al., 2013), but for which attribution of internal variability versus forced changes is challenging. Although this analysis focuses on CFC12, our findings are applicable to other transient oceanic tracers, such as CFC11, and SF6. Each ocean tracer has a unique atmospheric history, making some well suited for tracking recently ventilated waters, while others, like radiocarbon, can constrain longer timescales and deep ocean circulation (Gebbie & Huybers, 2012). All tracers are subject to internal variability that can influence our interpretation of ocean circulation changes.

These results have implications for the detectability of anthropogenic trends over internal variability. We present evidence that recent Southern Ocean circulation changes may be dominated by internal variability, rather than external forcing. Several other recent studies have also used a large ensemble approach to illustrate that anthropogenic changes in ocean circulation and biogeochemistry may be hard to detect on decadal timescales amidst relatively high internal variability (Brady et al., 2017, 2019; Freeman et al., 2018; Krumhardt et al., 2017; Long et al., 2016; McKinley et al., 2016, 2017; Negrete-García et al., 2019; Rodgers et al., 2015). Our study also focused on the decadal timescale, investigating only one pair of decadal surveys from 1991 to 2005. The results indicate that anthropogenic trends in ocean circulation in some regions will be only be detectable over periods longer than one or two decades.

The magnitudes of ΔpCFC12 variability we present are typically smaller than the steady circulation biases presented by other studies (Ting & Holzer, 2017; Waugh, 2014; Waugh et al., 2013). However, these other studies compare the observations to an assumed steady circulation model, while our results describe the

internal variability from the variable circulation CESM with respect to the large ensemble average, so the interpretation is not directly comparable. In this work, we conclude that ΔpCFC12 can be subject to high internal variability, but we do not specifically use ΔpCFC12 to diagnose circulation change. The magnitude in ideal age change variability we present is comparable to those from Tanhua et al., 2013, although a like for like comparison is difficult as they do not present results from P16S.

There are significant differences in the magnitude of age changes estimated using different tracer methods across previous studies. The 1-D transit time distribution (TTD) results presented in Waugh et al. (2013) show the largest inferred changes to upwelling and downwelling from pCFC12. However, Shao et al. (2016) recommend that 1-D TTDs should not be used to diagnose changes in ventilation in regions of strong upwelling, and the complex ventilation of AAIW means that the large ventilation changes in Waugh might be a result of systematic bias due to the oversimplification of the 1-D model. The data assimilation fixed circulation model from Waugh et al. (2013) shows a smaller tendency for change to upwelling in CDW and downwelling in most ocean basins in SAMW, closer to those we see in the CESM-LE. Ting and Holzer (2017) use a maximum entropy approach and multiple tracers, which constrain the TTD better than a 1-D approach. Again, the magnitudes of forced change they observe are smaller than the 1-D TTD, closer to those we see in the CESM-LE.

The simulations presented here are from a single low-resolution, non-eddy resolving model. Comparing against high-resolution ocean models, and ideally against high-resolution large ensembles, would give greater confidence in the magnitude of internal variability in ΔpCFC12 and ΔIAGE we present here and help quantify the impact of CESM's sluggish uptake of CFC12. Analysis of high-resolution models and model ensembles will help to determine if the anthropogenically forced trend or the internal variability in CESM-LE are biased, and if this leads to an overestimate of the relative influence of internal variability.

We chose to focus on the period before the CFC12 atmospheric concentration starts to decrease (approximately the year 2004) and where the amplitude of forcing is largest. We also chose to focus on a location and time period which had been studied in detail in the past and for which there are concurrent observations. Expanding the study to look at the ensemble-averaged interannual variability and trends could be the subject of further work. This analysis could be repeated using the historical experiments which carried IAGE and CFC12 from the 6th Coupled Model Intercomparison Project (CMIP6), to examine whether the conclusions here are representative of CESM only or are robust across models. Additionally, detection and attribution studies that investigate specific drivers, such as those included in Detection and Attribution Model Intercomparison Project (Gillett et al., 2016) as part of CMIP6, may help to refine estimates of the magnitude of internal variability in ocean circulation and biogeochemistry. We suggest that ocean tracers should be included in such detection and attribution studies in the future.

5. Conclusions

We have used an ensemble model approach to investigate the changes in observed pCFC12 over 1991 to 2005. The ensemble comprises members in which pCFC12 ventilation appears to have both increased and decreased in the water masses SAMW and CDW, purely through internal variability. When recalling the sluggish uptake of pCFC12 by CESM, ΔpCFC12 across the ensemble is consistent with the observations and of a similar magnitude to that observed in other studies which have found increases in upwelling and downwelling in the Southern Ocean. However, the changes in IAGE over the same period are largely dominated by internal variability, and the ensemble mean ΔIAGE is not significantly different from zero. The results suggest that inferred changes in ocean circulation over decadal timescales are likely dominated by internal processes rather than external forcing.

Acknowledgments
All data used for this analysis are publicly available. CESM ensemble output is available from the Earth System Grid (http://www.cesm.ucar.edu/projects/community-projects/LENS/data-sets.html). J. L. was supported by the Grantham Institute SSCP DTP, Grant NE/L002515/1 and the Imperial College London Stevenson Fund 2017. N. S. L. is grateful for support from the National Science Foundation (OCE-1752724 and OCE-1558225). CESM computing resources were provided by CISL at NCAR. We are indebted to the numerous sea-going and laboratory scientists that conducted the ocean CFC12 measurements and made their data available and to the GLODAPv2 project for gathering them into one data product. GLODAPv2 data were accessed online (at https://www.nodc.noaa.gov/ocads/oceans/GLODAPv2_2019/). We would also like to thank two anonymous reviewers for their constructive comments. This material is based upon work supported by the National Center for Atmospheric Research, which is a major facility sponsored by the National Science Foundation under Cooperative Agreement No. 1852977. Color maps used in this study are from Thyng et al. (2016). Natalie Freeman assisted with analysis of CESM-LE output.

References

Brady, R. X., Alexander, M. A., Lovenduski, N. S., & Rykaczewski, R. R. (2017). Emergent anthropogenic trends in California current upwelling. *Geophysical Research Letters*, *44*, 5044–5052. https://doi.org/10.1002/2017GL072945

Brady, R. X., Lovenduski, N. S., Alexander, M. A., Jacox, M., & Gruber, N. (2019). On the role of climate models in modulating the air–sea CO2 fluxes in eastern boundary upwelling systems. *Biogeosciences*, *16*, 329–346. https://doi.org/10.5194/bg-16-329-2019

Deser, C., Phillips, A., Bourdette, V., & Teng, H. (2012). Uncertainty in climate change projections: The role of internal variability. *Climate Dynamics*, *38*, 527–546. https://doi.org/10.1007/s00382-010-0977-x

Deser, C., Terray, L., & Phillips, A. S. (2016). Forced and internal components of winter air temperature trends over North America during the past 50 years: Mechanisms and implications. *Journal of Climate*, *29*, 2237–2258. https://doi.org/10.1175/JCLI-D-15-0304.1

DeVries, T., Holzer, M., & Primeau, F. (2017). Recent increase in oceanic carbon uptake driven by weaker upper-ocean overturning. *Nature*, *542*(7640), 215–218. https://doi.org/10.1038/nature21068

Fine, R. A. (2011). Observations of CFCs and SF6 as ocean tracers. *Annual Review of Marine Science*, *3*, 173–195. https://doi.org/10.1146/annurev.marine.010908.163933

Fine, R. A., Peacock, S., Maltrud, M. E., & Bryan, F. O. (2017). A new look at ocean ventilation time scales and their uncertainties. *Journal of Geophysical Research: Oceans*, *122*, 3771–3798. https://doi.org/10.1002/2016JC012529

Freeman, N. M., Lovenduski, N. S., Munro, D. R., Krumhardt, K. M., Lindsay, K., Long, M. C., & Maclennan, M. (2018). The variable and changing Southern Ocean Silicate Front: Insights from the CESM Large Ensemble. *Global Biogeochemical Cycles*, *32*, 752–768. https://doi.org/10.1029/2017GB005816

Fyke, J., Lenaerts, J. T. M., & Wang, H. (2017). Basin-scale heterogeneity in Antarctic precipitation and its impact on surface mass variability. *The Cryosphere*, *11*, 2595–2609. https://doi.org/10.5194/tc-11-2595-2017

Gebbie, G., & Huybers, P. (2012). The mean age of ocean waters inferred from radiocarbon observations: Sensitivity to surface sources and accounting for mixing histories. *Journal of Physical Oceanography*, *42*(2), 291–305. https://doi.org/10.1175/JPO-D-11-043.1

Gillett, N. P., Shiogama, H., Funke, B., Hegerl, G., Knutti, R., Matthes, K., et al. (2016). The Detection and Attribution Model Intercomparison Project (DAMIP v1.0) contribution to CMIP6. *Geoscientific Model Development*, *9*, 3685–3697. https://doi.org/10.5194/gmd-9-3685-2016

Gillett, N. P., & Thompson, D. W. (2003). Simulation of recent Southern Hemisphere climate change. *Science*, *302*(5643), 273–275. https://doi.org/10.1126/science.1087440

Graven, H. D., Gruber, N., Key, R., Khatiwala, S., & Giraud, X. (2012). Changing controls on oceanic radiocarbon: New insights on shallow-to-deep ocean exchange and anthropogenic CO2 uptake. *Journal of Geophysical Research*, *117*, C10005. https://doi.org/10.1029/2012JC008074

Hall, A., & Visbeck, M. (2002). Synchronous variability in the Southern Hemisphere atmosphere, sea ice, and ocean resulting from the annular mode. *Journal of Climate*, *15*, 3043–3057. https://doi.org/10.1175/1520-0442(2002)015<3043:SVITSH>2.0.CO;2

Kay, J. E., Deser, C., Phillips, A., Mai, A., Hannay, C., Strand, G., et al. (2015). The Community Earth System Model (CESM) large ensemble project: A community resource for studying climate change in the presence of internal climate variability. *Bulletin of the American Meteorological Society*, *96*(8), 1333–1349. https://doi.org/10.1175/BAMS-D-13-00255.1

Key, R. M., Olsen, A., van Heuven, S., Lauvset, S. K., Velo, A., Lin, X., et al. (2015). Global Ocean Data Analysis Project, Version 2 (GLODAPv2). ORNL/CDIAC-162, NDP-093. Carbon Dioxide Information Analysis Center, Oak Ridge National Laboratory, US Dept. of Energy, Oak Ridge, Tennessee. https://doi.org/10.3334/CDIAC/OTG.NDP093_GLODAPv2

Krumhardt, K. M., Lovenduski, N. S., Long, M. C., & Lindsay, K. (2017). Avoidable impacts of ocean warming on marine primary production: Insights from the CESM ensembles. *Global Biogeochemical Cycles*, *31*, 114–133. https://doi.org/10.1002/2016GB005528

Le Quéré, C., Rödenbeck, C., Buitenhuis, E. T., Conway, T. J., Langenfelds, R., Gomez, A., et al. (2007). Saturation of the Southern Ocean CO_2 sink due to recent climate change. *Science*, *316*, 1735–1738. https://doi.org/10.1126/science.1136188

Long, M. C., Deutsch, C., & Ito, T. (2016). Finding forced trends in oceanic oxygen. *Global Biogeochemical Cycles*, *30*, 381–397. https://doi.org/10.1002/2015GB005310

Long, M. C., Lindsay, K., & Peacock, S. (2013). Twentieth-century oceanic carbon uptake and storage in CESM1(BGC). *Journal of Climate*, *26*, 6775–6800. https://doi.org/10.1175/JCLI-D-12-00184.1

Lovenduski, N., & Gruber, N. (2005). Impact of the Southern Annular Mode on Southern Ocean circulation and biology. *Geophysical Research Letters*, *32*, L11603. https://doi.org/10.1029/2005GL022727

Lovenduski, N. S., Gruber, N., & Doney, S. C. (2008). Toward a mechanistic understanding of the decadal trends in the Southern Ocean carbon sink. *Global Biogeochemical Cycles*, *22*, GB3016. https://doi.org/10.1029/2007GB003139

Lovenduski, N. S., Gruber, N., Doney, S. C., & Lima, I. D. (2007). Enhanced CO2 outgassing in the Southern Ocean from a positive phase of the Southern Annular Mode. *Global Biogeochemical Cycles*, *21*, GB2026. https://doi.org/10.1029/2006GB002900

McKinley, G. A., Fay, A. R., Lovenduski, N., & Pilcher, D. J. (2017). Natural variability and anthropogenic trends in the ocean carbon sink. *Annual Review of Marine Science*, *9*, 125–150. https://doi.org/10.1146/annurev-marine-010816-060529

McKinley, G. A., Pilcher, D. J., Fay, A. R., Lindsay, K., Long, M. C., & Lovenduski, N. S. (2016). Timescales for detection of trends in the ocean carbon sink. *Nature*, *530*(7591), 469–472. https://doi.org/10.1038/nature16958

McLandress, C., Shepherd, T. G., Scinocca, J. F., Plummer, D. A., Sigmond, M., Jonsson, A. I., & Reader, M. C. (2011). Separating the dynamical effects of climate change and ozone depletion. Part II: Southern Hemisphere troposphere. *Journal of Climate*, *24*, 1850–1868. https://doi.org/10.1175/2010JCLI3958.1

Negrete-García, G., Lovenduski, N. S., Hauri, C., Krumhardt, K. M., & Lauvset, S. K. (2019). Sudden emergence of a shallow aragonite saturation horizon in the Southern Ocean. *Nature Climate Change*, *9*(4), 313–317. https://doi.org/10.1038/s41558-019-0418-8

Olsen, A., Key, R. M., van Heuven, S., Lauvset, S. K., Velo, A., Lin, X., et al. (2016). The Global Ocean Data Analysis Project version 2 (GLODAPv2)—An internally consistent data product for the world ocean. *Earth System Science Data*, *8*, 297–323. https://doi.org/10.5194/essd-8-297-2016

Polvani, L. M., Waugh, D. W., Correa, G. J. P., & Son, S.-W. (2011). Stratospheric ozone depletion: The main driver of twentieth-century atmospheric circulation changes in the southern hemisphere. *Journal of Climate*, *24*, 795–812. https://doi.org/10.1175/2010JCLI3772.1

Rintoul, S. R., & Naveira Garabato, A. C. (2013). Dynamics of the Southern Ocean circulation. In G. Siedler, S. Griffies, J. Gould, & J. Church (Eds.), *Ocean circulation and climate: A 21st century perspective*, *International Geophysics*, (2nd ed., Vol. 103, pp. 471–492). Oxford, GB: Academic Press.

Rodgers, K. B., Lin, J., & Frölicher, T. L. (2015). Emergence of multiple ocean ecosystem drivers in a large ensemble suite with an Earth system model. *Biogeosciences*, *12*, 3301–3320. https://doi.org/10.5194/bg-12-3301-2015

Russell, J. L., Dixon, K. W., Gnanadesikan, A., Stouffer, R. J., & Toggweiler, J. R. (2006). The southern hemisphere westerlies in a warming world: Propping open the door to the deep ocean. *Journal of Climate*, *19*, 6382–6390. https://doi.org/10.1175/JCLI3984.1

Shao, A. E., Mecking, S., Thompson, L. A., & Sonnerup, R. E. (2016). Evaluating the use of 1-D transit time distributions to infer the mean state and variability of oceanic ventilation. *Journal of Geophysical Research: Oceans*, *121*, 6650–6670. https://doi.org/10.1002/2016JC011900

Smith, R., Jones, P., Briegleb, B., Bryan, F., Danabasoglu, G., Dennis, J., et al. (2010). The parallel ocean program (POP) reference manual: Ocean component of the community climate system model (CCSM) and community earth system model (CESM) 1. Tech. Rep. LA-UR-10-01853, Los Alamos Natl. Lab., Los Alamos, N. M. 23 March 2010.

Talley, L. D., Feely, R. A., Sloyan, B. M., Wanninkhof, R., Baringer, M. O., Bullister, J. L., et al. (2016). Changes in ocean heat, carbon content, and ventilation: A review of the first decade of GO-SHIP global repeat hydrography. *Annual Review of Marine Science*, *8*, 185–215. https://doi.org/10.1146/annurev-marine-052915-100829

Tanhua, T., Waugh, D. W., & Bullister, J. L. (2013). Estimating changes in ocean ventilation from the early 1990s CFC-12 and late SF6 measurements. *Geophysical Research Letters*, *40*, 927–932. https://doi.org/10.1002/grl.50251

Thompson, D. W. J., Solomon, S., Kushner, P. J., England, M. H., Grise, K. M., & Karoly, D. J. (2011). Signatures of the Antarctic ozone hole in Southern Hemisphere surface climate change. *Nature Geoscience*, *4*, 741–749. https://doi.org/10.1038/NGEO1296

Thyng, K. M., Greene, C. A., Hetland, R. D., Zimmerle, H. M., & DiMarco, S. F. (2016). True colors of oceanography: Guidelines for effective and accurate colormap selection. *Oceanography*, *29*(3), 9–13. https://doi.org/10.5670/oceanog.2016.66

Ting, Y.-H., & Holzer, M. (2017). Decadal changes in the Southern Ocean ventilation inferred from deconvolutions of repeat hydrographies. *Geophysical Research Letters*, *44*, 5655–5664. https://doi.org/10.1002/2017GL073788

Warner, M. J., & Weiss, R. F. (1985). Solubilities of chlorofluorocarbons 11 and 12 in water and seawater. *Deep Sea Research*, *32*(12), 1485–1497. https://doi.org/10.1016/0198-0149(85)90099-8

Waugh, D. W. (2014). Changes in the ventilation of the southern oceans. *Philosophical Transactions of the Royal Society A*, *372*. https://doi.org/10.1098/rsta.2013.0269

Waugh, D. W., Hogg, A. M., Spence, P., England, M., & Haine, T. (2019). Response of Southern Ocean ventilation to changes in midlatitude westerly winds. *Journal of Climate*, *32*, 5345–5361. https://doi.org/10.1175/JCLI-D-19-0039.1

Waugh, D. W., Primeau, F., DeVries, T., & Holzer, M. (2013). Recent changes in the ventilation of the southern oceans. *Science*, *339*(6119), 568–570. https://doi.org/10.1126/science.1225411